Original Article

Minimal Impact of a De Novo–Expressed β-Cell Autoantigen on Spontaneous Diabetes Development in NOD Mice

Marianne M. Martinic,[1] Amy E. Juedes,[1] Damien Bresson,[1] Dirk Homann,[2] Kresten Skak,[3] Christoph Huber,[4] Eleanor Ling,[1] Mette Ejrnaes,[1] Tom Wolfe,[1] Lisa Togher,[1] Urs Christen,[5] and Matthias G. von Herrath[1]

During an autoimmune process, the autoaggressive response spreads from the initiating autoantigen to other antigens expressed in the target organ. Based on evidence from experimental models for multiple sclerosis, such "antigenic spreading" can play an important role in the exacerbation of clinical disease. We evaluated whether pathogenesis of spontaneous diabetes in NOD mice could be accelerated in a similar way when a novel autoantigen was expressed in pancreatic β-cells. Unexpectedly, we found that the expression of the lymphocytic choriomeningitis virus nucleoprotein only led to marginal enhancement of diabetes, although such NOD-nucleoprotein mice were not tolerant to nucleoprotein. Although the frequency of nucleoprotein-specific CD8 T-cells in the pancreatic draining lymph node was comparable with the frequency of islet-specific glucose-6-phosphatase catalytic subunit-related protein (IGRP)-specific T-cells, more IGRP-specific CD8 T-cells were found both systemically and in the islets where there was a fourfold increase. Interestingly, and in contrast to nucleoprotein-specific CD8 T-cells, IGRP-specific T-cells showed increased CXCR3 expression. Thus, autoreactivity toward de novo–expressed β-cell autoantigens will not accelerate autoimmunity unless large numbers of antigen-experienced autoreactive T-cells expressing the appropriate chemokine receptors are present.
***Diabetes* 56:1059–1068, 2007**

From the [1]Division of Developmental Immunology, La Jolla Institute for Allergy and Immunology, La Jolla, California; the [2]Barbara Davis Center for Childhood Diabetes, University of Colorado at Denver and Health Sciences Center, Aurora, Colorado; [3]Pharmacology Research, Novo Nordisk A/S, Måløv, Denmark; the [4]Department of Immunology, The Scripps Research Institute, La Jolla, California; and [5]Klinik der Johann Wolfgang Goethe Universität, Frankfurt, Germany.

Address correspondence and reprint requests to Marianne M. Martinic or Matthias G. von Herrath, Immune Regulation Lab DI-3, La Jolla Institute for Allergy and Immunology, 9420 Athena Circle, La Jolla, CA 92037. E-mail: marmar@liai.org or matthias@liai.org.

Received for publication 14 January 2005 and accepted in revised form 22 November 2006.

M.M.M. and A.E.J. contributed equally to this work.

CTL, cytotoxic T-lymphocyte; CNS, central nervous system; EAE, experimental autoimmune encephalomyelitis; ELISA, enzyme-linked immunosorbent assay; GAD, glutamic acid decarboxylase; HBS, hepatitis B virus polyadenylation signal; IFN-γ, γ-interferon; IGRP, islet-specific glucose-6-phosphatase catalytic subunit-related protein; IL, interleukin; LCMV, lymphocytic choriomeningitis virus; MHC, major histocompatibility complex; PBS-T, 0.05% Tween 20 in PBS; PDLN, pancreatic draining lymph node; pfu, plaque forming unit; RIP, rat insulin promoter.

DOI: 10.2337/db05-0062

Elegant studies (1,2) have established an important role for antigenic spreading in the Theiler's virus and experimental autoimmune encephalomyelitis (EAE) models for inflammatory central nervous system (CNS) disease/multiple sclerosis. Such experiments showed that uptake and presentation of CNS antigens occur after virally induced inflammation and are responsible for recurrence of disease in the EAE model (3). Antigenic and epitope spreading also occurs in autoimmune diabetes and has been analyzed extensively in the NOD mouse model for spontaneous type 1 diabetes (4). Sercarz and colleagues (5) have described unmasking of cryptic and other determinants located on the islet antigen glutamic acid decarboxylase (GAD). The new epitopes are targeted by autoreactive CD4 lymphocytes that can have either aggressive or regulatory effector phenotypes as evidenced by their cytokine production (5). However, there is no clear knowledge about their precise impact on the spontaneous disease process, and studies comparable with the Miller investigations in multiple sclerosis models (3) were not possible in the NOD mouse because the disease course is not relapsing/remitting.

Kaufman and colleagues (6) have described "infectious spreading" of T_H1 or T_H2 immunity, a phenomenon that is also acknowledged in other models. It has been demonstrated that after therapeutic intervention, the resultant regulatory T-cells operate through the production of the immunomodulatory cytokines interleukin (IL)-4 and IL-10 (7–9). In these studies, type 1 diabetes–protected NOD mice exhibited T_H2 responses to several islet antigens such as insulin and GAD, whereas nonprotected mice produced γ-interferon (IFN-γ) in parallel assays (8). Again, functional analysis of these responses could be performed in vitro or in transfers but not directly in the disease process. It is well known that initially, insulin-B–specific CD8 lymphocytes are generated in islets of NOD mice (10), but they do not directly correlate with disease and even disappear later during the pre-diabetic phase (11). However, proinsulin and more precisely insB9-23 peptide appear to be a major autoantigen in NOD mice (12,13). In addition, CD8 cells specific for the NRP-7 peptide reactive to the autoantigen islet-specific glucose-6-phosphatase catalytic subunit-related protein (IGRP) (14) arise in waves during NOD type 1 diabetes pathogenesis (15). These cells have strong pathogenic potential in T-cell receptor transgenic mice (16), and tolerance to NRP-7 alleviates type 1

diabetes (17). Overall, it is still unclear whether antigenic spreading plays a pathogenic role in the NOD disease process or whether some initially generated pathogenic driver clones are the sole culprits (10,12,15,18). This issue is of course of therapeutic interest, because if we intend to re-establish tolerance to β-cells, we must be sure that we are eliminating aggressive T-cells specific to the most relevant epitopes.

We therefore chose to address this important problem from the antigenic side by investigating whether constitutive expression of a de novo autoantigen in pancreatic β-cells would have a significant impact on the course of diabetes in NOD mice. We used the human insulin promoter to express the nucleoprotein of lymphocytic choriomeningitis virus (LCMV) directly in NOD pancreatic β-cells. Previous studies had already shown the successful generation of rat insulin promoter (RIP)-LCMV-nucleoprotein H-2^b (B6-nucleoprotein) and H-2^d (BALB/c-nucleoprotein) transgenic mice and complete tolerance to the nucleoprotein had never been observed despite the fact that thymic expression of nucleoprotein in some of the transgenic lines had eliminated high avidity nucleoprotein-specific CD8 T-cells (19).

Infection of NOD-nucleoprotein transgenic lines with LCMV induced very rapid diabetes within 2 weeks, in this way establishing proof that autoreactivity to nucleoprotein can be highly pathogenic. In contrast, spontaneous diabetes in NOD-nucleoprotein mice was only marginally accelerated, despite the fact that the frequency of nucleoprotein-specific CD8 T-cells was comparable with those specific for the autoantigen IGRP in the pancreatic draining lymph nodes (PDLNs). However, the systemic load of spontaneously arising IGRP-specific CD8 T-cells was severalfold higher than those specific for nucleoprotein. In addition, IGRP-specific CD8 T-cells accumulated to fourfold higher levels in the pancreas and showed increased CXCR3 expression. Therefore, autoreactivity to de novo–expressed β-cell autoantigens will not necessarily accelerate autoimmunity, unless high systemic numbers of activated autoantigen-specific T-cells expressing the appropriate chemokine receptors are present. The profound drive of viral inflammation in LCMV-infected NOD-nucleoprotein mice provides just such an environment.

RESEARCH DESIGN AND METHODS

Transgenic RIP-LCMV-GP H-2^b (B6-GP), RIP-LCMV-nucleoprotein H-2^b (B6-nucleoprotein) (backcross F_{10-12} to C57BL/6J), and RIP-LCMV-nucleoprotein H-2^d (BALB/c-nucleoprotein) mice expressing LCMV-glycoprotein (GP) or -nucleoprotein in their pancreatic β-cells, respectively, and for the B6-nucleoprotein and BALB/c-nucleoprotein line also in the thymus, were previously generated and characterized in our laboratory (19). Screening was performed by Southern blot and PCR as described previously (19). C57BL/6J (B6), BALB/c, and NOD Lt/J (NOD) mice were obtained from The Jackson Laboratories (Bar Harbor, ME).

Generation of NOD-nucleoprotein transgenic mice. The complete cDNA gene for the LCMV-nucleoprotein coding regions was assembled from overlapping cDNA clones derived from the S RNA segment of LCMV (ARM clone 53b) (20). The LCMV-nucleoprotein cDNA was cloned into the Ins-plasmid as *Bam*HI fragment. The Ins-plasmid contains the human insulin promoter (Ins) and the Hepatitis B virus polyadenylation signal (HBS) as a terminator of transcription. Transgenic Ins-LCMV-nucleoprotein NOD mice (NOD-nucleoprotein) were generated at the Scripps Transgenic and Embryonic Steam Cell core facility. Briefly, the *Sac*I/*Hin*dIII linearized Ins-LCMV-nucleoprotein-HBS gene construct was microinjected into one of the pronuclei of fertilized NOD mouse eggs, which were subsequently implanted into the oviduct of pseudopregnant recipient NOD mice. Offspring were screened for presence of the transgene by PCR and slot blot hybridization. The primers nucleoprotein-sense (5′-CAGTTATAGGTGCTCTTCGC) and nucleoprotein-antisense (5′-AG ATCTGGGAGCCTTGCTTTG) were used for the amplification of transgenic LCMV-nucleoprotein from mouse-tail DNA yielding a 289-bp PCR product (19). Slot blot hybridization was performed as described elsewhere (20) using a radiolabeled LCMV-nucleoprotein–specific probe.

RT-PCR. Organs were snap-frozen and homogenized in Trizol reagent (Invitrogen), and total RNA was extracted. To prevent its degradation, pancreatic RNA was re-extracted a second time to ensure complete removal of RNases. Residual genomic DNA was eliminated by DNase digestion for 20 min with the TURBO-DNAfree kit (Ambion). Reverse transcription was carried out with 5 μg total RNA using the first-strand cDNA synthesis kit (Amersham Biosciences) with the oligo dT-primer provided in the kit according to the manufacturer's instructions. PCR primers were as follows: β-actin, 5′ GACG GCCAGGTCATCACTAT 3′ and 5′ ACATCTGCTGGAAGGTGGAC 3′; and nucleoprotein, 5′ CAGTTATAGGTGCTCTTCGC 3′ and 5′ AGATCTGGGAGC CTTGCTTTG 3′.

Enzyme-linked immunosorbent assay for detection of insulin and LCMV-nucleoprotein proteins. Thymus, pancreas, and brain were obtained from 6- to 8-week-old B6-nucleoprotein ($n = 4$), NOD-nucleoprotein ($n = 4$), and NOD ($n = 4$) mice. Pancreatic islets were isolated using a Ficoll gradient as previously described (21). Proteins from each organ were extracted from the tissues using the T-PER tissue protein extraction reagent (Pierce) as recommended by the manufacturer. Extracted proteins were used in an enzyme-linked immunosorbent assay (ELISA) as follows. Briefly, the wells were coated overnight at 4°C with 10 or 100 μg/ml proteins diluted in 1× PBS and extracted from the pancreatic islets or the thymus, respectively. Brain protein extracts were coated at both 10 and 100 μg/ml in 1× PBS. The wells were washed with 0.05% Tween 20 in PBS (PBS-T) and blocked with 2% BSA in PBS-T (saturation buffer) for 1 h at 37°C. After three washings, rabbit polyclonal anti-LCMV antibody (22) or guinea pig polyclonal anti-insulin antibody (Dako) both diluted 1:2,000 in saturation buffer were incubated for 2 h at 37°C. After three washings, biotinylated anti-rabbit or anti–guinea pig secondary antibodies (dilution 1:2,000) were added to the wells in saturation buffer for 1 h at 37°C. After washings, horseradish peroxidase–conjugated avidin (dilution 1:2,000; Vector Laboratories, Burlingame, CA) was used for 1 h at 37°C. The reactivity was revealed by using the 2,2′-azino-bis-[3-ethylbenzthiazoline-6-sulfonic acid] substrate (Sigma, St. Louis, MO). The absorbance was measured at 405 nm after 30 min.

Blood glucose assessments. Blood glucose values were determined using OneTouch Ultra (LifeScan, Milpitas, CA). Unless otherwise indicated, mice with blood glucose values >300 mg/dl were considered diabetic.

Viruses. LCMV Armstrong clone 53b (LCMV) prepared by a single passage on BHK-21 cells was used throughout experiments. Unless otherwise indicated, mice were infected with a single dose of 1×10^5 plaque forming units (pfu) i.p.

Cytotoxic T-lymphocyte assays. Cytotoxic T-lymphocyte (CTL) activity was measured in a standard 5- to 6-h ex vivo ^{51}Cr release assay as described (23). In brief, MC57 (H-2D^b–positive fibroblast cell line), syngeneic NIT (β-cell insulinoma cell line, H-2^{g7}), or allogeneic BALB/c (H-2^d) target cells were infected with LCMV (multiplicity of infection = 0.1) or pulsed with major histocompatibility complex (MHC) class I–restricted LCMV peptides (10^{-5} mol/l). Assays using effector splenic lymphocytes at days 7 or 8 after infection used effector to target ratios of 50:1, 25:1, and 12.5:1, and those using CTL clones used ratios of 5:1 and 2.5:1.

Isolation of lymphocytes from the pancreas. Pancreata were dissected, and PDLNs were carefully removed. Pancreata were mechanically disrupted using glass slides. Material was pooled from two to five mice, and the lymphocytes were separated using a lympholyte gradient (CedarLane).

Flow cytometry. Flow cytometry antibodies were purchased from BD Pharmingen (San Diego, CA), eBioscience (San Diego, CA), Caltag Laboratories (Burlingame, CA), and R&D Systems (Minneapolis, MN). Single-cell suspensions were stained with MHC class I tetramers and fluorescein isothiocyanate–conjugated anti-CD8 antibody for 30 min at 4°C. For multicolor fluorescence-activated cell sorter analysis, single-cell suspensions were first stained with MHC class I tetramers for 15 min at room temperature and then with the antibody mix for 20 min at 4°C. Afterward, cells were washed and fixed in 2% paraformaldehyde. For intracellular stains, single-cell suspensions were restimulated for 5–6 h with NP396 or NRP-V7 peptide in the presence of brefeldin A (Sigma). Cells were stained for surface expression of CD8, CD3, CD44, and CD62L and were then fixed, permeabilized, and stained for intracellular IFN-γ and TNF. Samples were acquired either on a FACSCalibur or LSRII flow cytometer and analyzed using CellQuest (BD Biosciences, San Jose, CA) or FlowJo (version 8.1.1; Tree Star, Ashland, OR) software. The following MHC class I tetramers were used: H-2D^b refolded with the LCMV peptide NP396 (FQPQNGQFI) (24), or H-2K^d refolded with the NRP-V7 peptide (KYNKANVFL) or the negative control peptide TUM (KYQAVTTTL) (17). NRP-V7 tetramers were a kind gift of Rusung Tan (Vancouver, Canada).

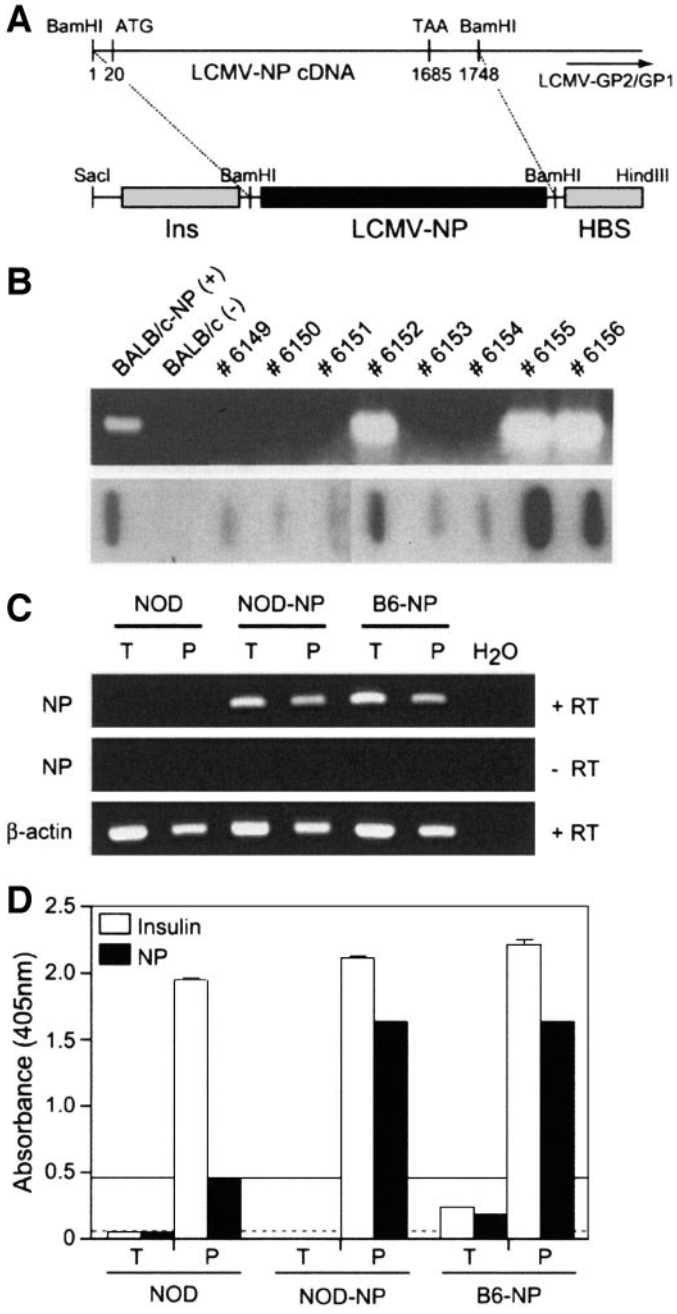

FIG. 1. Generation and screening of NOD-nucleoprotein transgenic mice. *A*: The LCMV-nucleoprotein cDNA was cloned into the Ins-plasmid as *Bam*HI fragment. The Ins-plasmid contains the human insulin promoter (Ins) and the HBS as a terminator of transcription. The *Sac*I/*Hin*dIII linearized Ins-LCMV-nucleoprotein-HBS gene construct was microinjected into one of the pronuclei of fertilized NOD mouse eggs, which were subsequently implanted into the oviduct of pseudo-pregnant recipient NOD mice. *B*: Offspring (6149–6156) were screened for presence of the transgene by PCR and Slot blot hybridization. Genomic DNA of a BALB/c-nucleoprotein and wild-type BALB/c mouse were used as positive and negative control, respectively. The resulting 289-bp PCR product is displayed (*top*). Slot blot hybridization was performed using a radiolabeled LCMV-nucleoprotein–specific probe (*bottom*). *C*: RT-PCR analysis of LCMV-nucleoprotein (NP) and β-actin transcripts expressed in the thymus (T) and pancreas (P) of NOD (negative control), NOD-nucleoprotein (line 6171), and B6-nucleoprotein (positive control) mice. Samples were run with (+RT) or without reverse transcriptase (−RT). *D*: The expression levels of insulin (white bars) and LCMV-nucleoprotein (NP, black bars) proteins were assessed by ELISA in the thymus (T) and pancreatic islets (P) of NOD (negative control), NOD-nucleoprotein (line 6171), and B6-nucleoprotein (positive control) mice. The data are given in absorbance after subtraction of the background values corresponding to the absorbance observed with proteins extracted from the brain of each mouse strains. Results are expressed as means ± SD of duplicate values. Lines indicate the detection limit for nucleoprotein protein in the thymus (dashed line) and pancreatic islets (solid line).

Immunocytochemistry. Tissues were immersed in Tissue-Tek OCT compound (Sakura Finetek USA, Torrance, CA) and quick-frozen on dry ice. Six- to 10-μm cryomicrotome tissue sections were affixed to sialin-coated Superfrost Plus slides (Fisher Scientific, Pittsburgh, PA). Sections were fixed with 95% EtOH at −20°C and washed in PBS, and then endogenous avidin-biotin was blocked using the avidin/biotin blocking kit from Vector Laboratories. Primary anti-mouse CD8 (Pharmingen) and biotinylated secondary antibodies (Vector Laboratories) were incubated with the sections, and the color reaction was obtained by sequential incubation with avidin-peroxidase conjugate (Vector Laboratories) and diaminobenzidine–hydrogen peroxide.

Generation of NP396- and GP33-specific NOD T-cell clones. The generation and maintenance of LCMV-specific T-cell clones in long-term cultures have been previously described (25,26). In brief, the NP396-specific NOD T-cell clone 9-A-8 and the GP33-specific NOD T-cell clone 13-G-8 were isolated from LCMV-infected NOD recipients and stimulated frequently with irradiated NP396 or GP33 peptide-loaded syngeneic macrophages, respectively, and recombinant human IL-2 (20 units/ml).

RESULTS

Immunity to LCMV-nucleoprotein expressed in islets of NOD-nucleoprotein transgenic mice leads to rapid diabetes after LCMV infection. NOD-nucleoprotein transgenic mice expressing the LCMV-nucleoprotein in pancreatic β-cells were generated directly on the NOD background (Fig. 1*A*). Four NOD-nucleoprotein transgenic lines (lines 6152, 6156, 6159, and 6171) were established (Fig. 1*B*; data not shown). Mice derived from lines 6152 and 6171 expressed LCMV-nucleoprotein in the pancreas and in the thymus (Fig. 1*C* and *D*; data not shown); lines 6156 and 6159, however, did not express LCMV-nucleoprotein in the pancreas (data not shown). The expression of LCMV-nucleoprotein in the pancreas correlated with the speed of diabetes induction after infection with LCMV. In fact, only mice expressing nucleoprotein in the pancreas (derived from lines 6152 and 6171) were susceptible to LCMV-induced diabetes (Fig. 2*A*). Pancreata from these mice analyzed by immunohistochemistry 1 week after infection with LCMV also revealed the early infiltration of islets by CD8 T-cells (Fig. 2*B*).

Diabetes in the new NOD-nucleoprotein transgenic mice occurred rapidly within 2 weeks of infection with LCMV (Fig. 2*A*), compared with the slow onset (3–6 months) in B6-nucleoprotein mice (19). The rapid onset of diabetes in NOD-nucleoprotein transgenic mice correlated well with the comparatively higher frequency of NP396-specific T-cells, which made up 2% of CD8 T-cells in NOD-nucleoprotein versus 0.8% in B6-nucleoprotein lines (Table 1). Despite the rapid onset of diabetes, NOD-nucleoprotein transgenic mice did exhibit some degree of tolerance to the nucleoprotein antigen, as evidenced by the lower NP396-specific CD8 T-cell frequency and cytotoxic activity compared with NOD nontransgenic mice (Table 1). Because nucleoprotein is expressed in the thymus of NOD-nucleoprotein transgenic mice (Fig. 1*C*), nucleoprotein-specific tolerance could be explained by thymic deletion of high avidity nucleoprotein-specific CD8 T-cells. Similar observations have already been made for B6-nucleoprotein transgenic mice (19). In addition, other tolerance mechanisms, such as peripheral tolerance, may also be involved in deletion of nucleoprotein-specific CD8 T-cells.

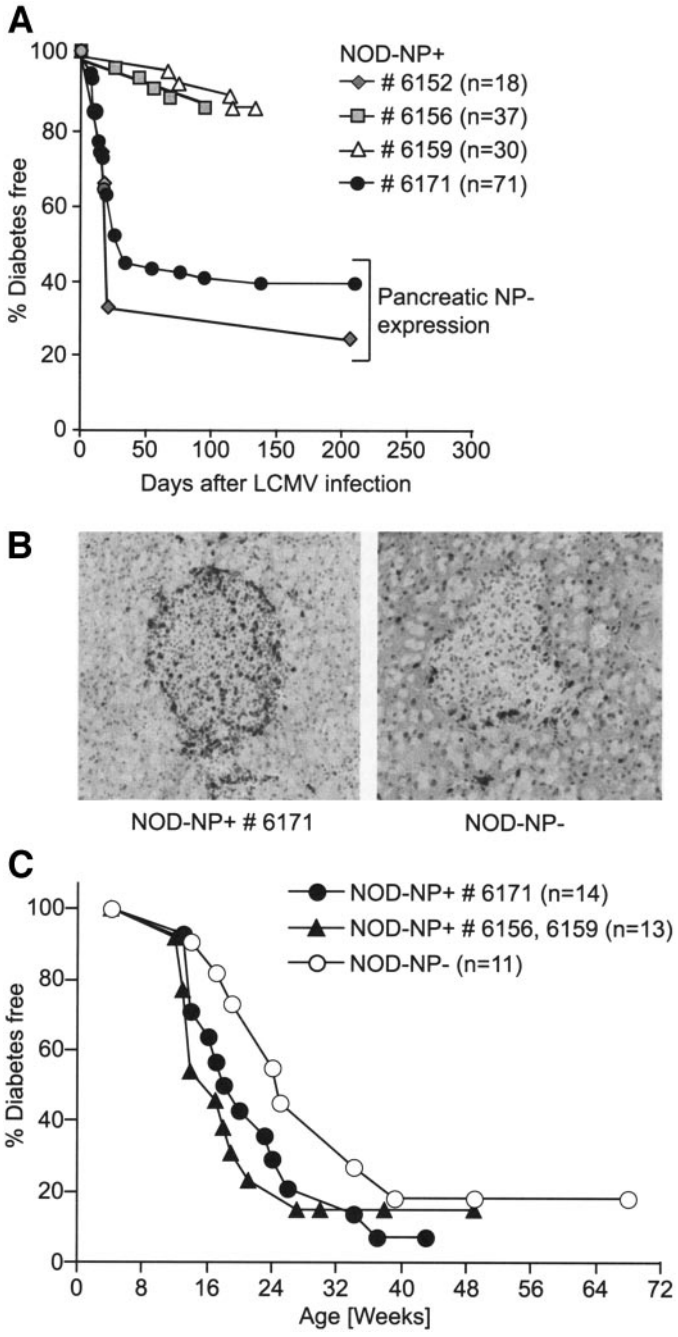

FIG. 2. In NOD-nucleoprotein transgenic mice, diabetes is accelerated only after infection with LCMV. *A*: Groups of 6- to 8-week-old NOD-nucleoprotein transgenic mice from four founder lines (lines 6152, 6156, 6159, and 6171) were infected with 1×10^5 pfu LCMV i.p. Only mice derived from lines 6152 and 6171 expressed LCMV-nucleoprotein in the pancreas. Blood glucose values were measured weekly, and the percentage of mice that remained diabetes free was determined. *B*: Pancreata from NOD-nucleoprotein transgenic mice expressing nucleoprotein in the pancreas (NOD-nucleoprotein$^+$, line 6171) and from transgene-negative littermates (NOD-nucleoprotein$^-$) were harvested 7 days after infection with LCMV. Tissue sections were stained for the presence of CD8 T-cells. *C*: Spontaneous incidence of type 1 diabetes was determined in naive NOD-nucleoprotein transgenic females with (line 6171, black circles) or without (line 6156 and 6159, black triangles) pancreatic nucleoprotein expression, and in naive transgene-negative littermates (NOD-nucleoprotein$^-$, white circles). Mice were considered diabetic when blood glucose levels were >300 mg/dl.

Marginal acceleration of spontaneous diabetes occurs in NOD-nucleoprotein transgenic females expressing the nucleoprotein autoantigen in β-cells. The precise time course of spontaneous diabetes development in NOD-nucleoprotein transgenic females with (derived from line 6171) or without pancreatic nucleoprotein expression (derived from lines 6156 and 6159), and in transgene-negative littermates (NOD-nucleoprotein$^-$) was followed to understand the impact of the de novo–expressed nucleoprotein islet antigen on the spontaneous disease. Interestingly, overall incidence of diabetes was not significantly increased (log-rank test, $P < 0.1392$), and the kinetics of development were only slightly accelerated (Fig. 2*C*). Thus, expression of the foreign nucleoprotein antigen in pancreatic β-cells only had a minimal impact on the course of spontaneous diabetes development in NOD-nucleoprotein transgenic mice. This was surprising because NOD-nucleoprotein mice did not exhibit complete tolerance to nucleoprotein (Table 1) and rapid induction of diabetes had occurred after LCMV infection (Fig. 2*A*), demonstrating that there were no other defects or epigenetic phenomena that would prevent destruction of β-cells in these mice.

Comparable frequencies of autoaggressive CD8 T-cells specific for the neo-autoantigen nucleoprotein and autoantigen IGRP are found in the pancreatic lymph nodes of NOD-nucleoprotein$^+$ transgenic mice. We next determined whether introduction of nucleoprotein into the spontaneous autoimmune process in NOD mice would result in the accumulation of nucleoprotein-specific CD8 lymphocytes. NP396-specific CD8 lymphocytes were therefore isolated at different time points from the PDLNs and spleens during spontaneous diabetes development and enumerated by NP396/D^b tetramer staining (Fig. 3*A* and *B*). As expected, NP396-specific CD8 T-cells were not detected in the PDLNs or spleens of transgene-negative littermates (NOD-nucleoprotein$^-$) (Fig. 3*A* and *B*, white circles). However, in NOD-nucleoprotein transgenic mice expressing nucleoprotein in the pancreas (NOD-nucleoprotein$^+$, derived from line 6171) NP396-specific CD8 T-cells were detected in the PDLNs but not the spleens (Fig. 3*A* and *B*, black circles). NP396-specific T-cells were found in the PDLNs of 9 of 13 mice between 13 and 18 weeks of age and were less frequently detected (2 of 9 mice) in 9-week-old NOD-nucleoprotein$^+$ mice (Fig. 3*A*). The frequency of NP396-specific CD8 T-cells in the PDLN was quite low (0.3–0.7% NP396/D^b tetramer$^+$ CD8 T-cells) compared with the frequencies arising after systemic LCMV infection (2–3% of CD8 T-cells; data not shown). In addition, not all mice examined had detectable NP396-specific CD8 T-cells (Fig. 3*A*).

The frequency of NP396-specific CD8 T-cells was then compared with those specific for another autoantigen, IGRP, as detected by NRP-V7/K^d tetramer staining (Fig. 3*C* and *D*). The average frequencies of NRP-V7– and NP396-specific CD8 T-cells in the PDLNs of 13- to 18-week-old mice were very similar, representing 0.52 and 0.54% of CD8 T-cells, respectively. However, NRP-V7–specific CD8 T-cells were found in a higher proportion of NOD (NOD-nucleoprotein$^+$ and NOD-nucleoprotein$^-$) mice, especially at early time points during diabetes development (nine of nine mice with NRP-V7/K^d tetramer$^+$ staining at 9 weeks of age) (Fig. 3*C*). In addition, NRP-V7– but not NP396-specific CD8 T-cells were found systemically in the spleen of NOD-nucleoprotein$^+$ and NOD-nucleoprotein$^-$ mice (Fig. 3*D*), as reported previously (15).

Increased systemic frequencies of NRP-V7– versus NP396-specific CD8 T-cells in the spleen correlate with increased islet infiltration and increased CXCR3

TABLE 1
Systemic generation of NP396-specific CD8 T-cells in NOD-nucleoprotein$^+$ transgenic mice

Transgenic line	Nucleoprotein expression	NP396-specific cytotoxic T-cell activity*	NP396-specific CD8 T-cell frequency†	Diabetes (LCMV)‡
NOD-nucleoprotein	Pancreas and thymus	36 ± 10	2.0	10–14 days
B6-nucleoprotein	Pancreas and thymus	12 ± 3	0.8	3–6 months (19)
NOD	None	53 ± 9	5.5	None (24)

Data are means ± SD (%). NOD-nucleoprotein$^+$ transgenic mice, expressing nucleoprotein in pancreatic β-cells, were derived from line 6171. Groups of three mice were infected with 10^5 pfu LCMV i.p. Seven days later, spleens were harvested, and CTL activity and frequency of NP396-specific CD8 T-cells were determined. *CTL activity was determined directly in an ex vivo ^{51}Cr-release assay using NP396 peptide–labeled MC57 (H-2D^b) target cells. The data shown are for 50:1 effector:target ratio. †NP396-specific CD8 T-cell frequencies were analyzed by gating on CD8 T-cells and determining the percentage of NP396/D^b tetramer$^+$ CD8 T-cells. Numbers represent the average of the three mice per group. ‡The time frame after which the majority of the transgenic mice developed diabetes after LCMV infection is indicated.

expression by NRP-V7–specific CD8 T-cells. Although the frequency of NP396– or NRP-V7–specific CD8 T-cells in the PDLNs was relatively low (Fig. 3), these cells were enriched in the pancreas itself (Fig. 4*A*). Lymphocytes were isolated from pooled pancreas samples from naive NOD-nucleoprotein transgenic mice expressing nucleoprotein in the pancreas (NOD-nucleoprotein$^+$, derived from line 6171) or nontransgenic littermates (NOD-nucleoprotein$^-$). The frequency of NP396– and NRP-V7–specific CD8 T-cells in the pancreas was much higher than in the PDLNs (Figs. 4*A* and 3*A* and *C*). However, NRP-V7–specific CD8 T-cells accumulated in the pancreas to fourfold higher levels than NP396-specific T-cells (Fig. 4*A*).

To analyze whether the increased accumulation of NRP-V7–specific T-cells in the pancreas was paralleled

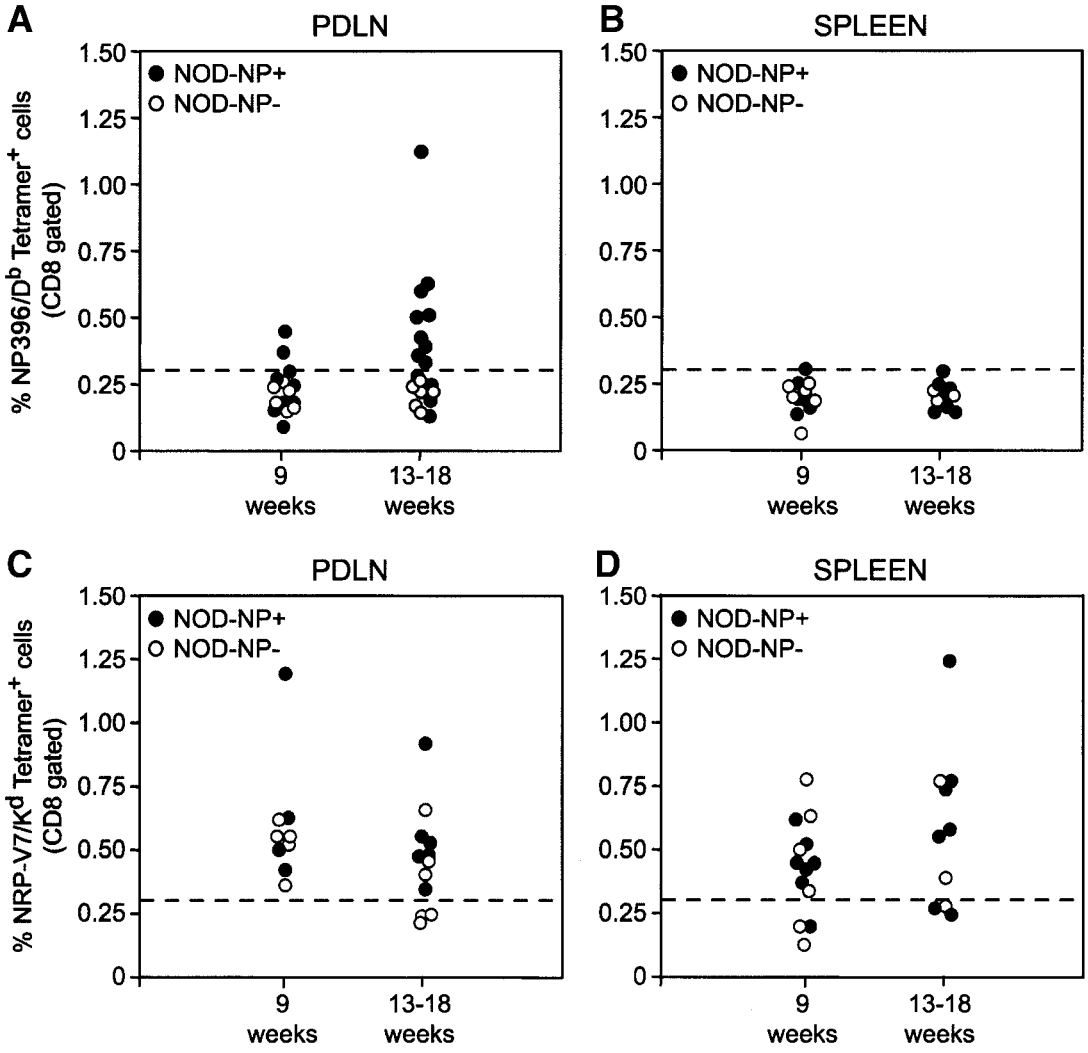

FIG. 3. NP396-specific CD8 T-cells are detected in pancreatic draining lymph nodes but not in spleens of NOD-nucleoprotein$^+$ transgenic mice. PDLNs (*A* and *C*) and spleens (*B* and *D*) from NOD-nucleoprotein transgenic mice expressing nucleoprotein in the pancreatic islets (NOD-nucleoprotein$^+$, line 6171, black circles) and from transgene-negative littermates (NOD-nucleoprotein$^-$, white circles) were isolated at the indicated time points. NP396– and NRP-V7–specific CD8 lymphocytes were enumerated by NP396/D^b (*A* and *B*) and NRP-V7/K^d (*C* and *D*) tetramer staining, respectively. The percentage of antigen-specific cells within gated CD8$^+$ populations is graphed for individual mice.

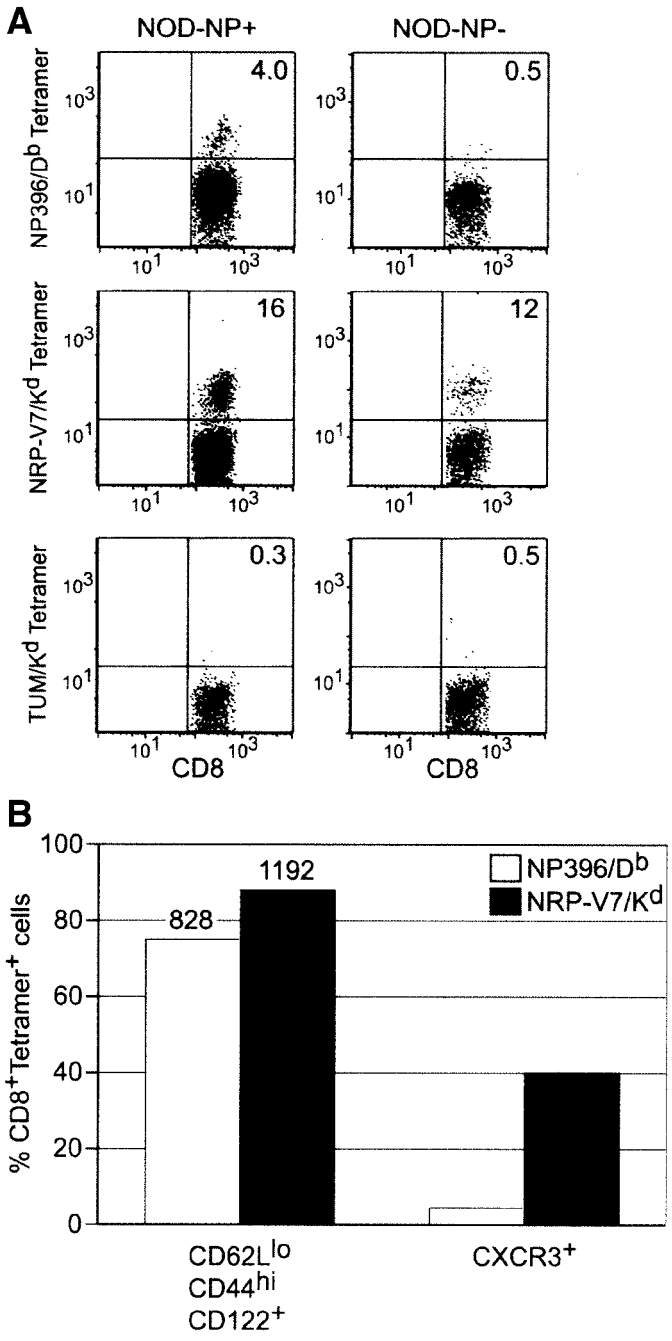

FIG. 4. NP396-specific CD8 T-cells are enriched in the pancreas of pre-diabetic NOD-nucleoprotein$^+$ transgenic mice and show an activated phenotype. *A*: Lymphocytes isolated from the pancreas of groups of three to four pre-diabetic NOD-nucleoprotein transgenic mice expressing nucleoprotein in the pancreas (NOD-nucleoprotein$^+$, line 6171, *left column*) or from transgene-negative littermates (NOD-nucleoprotein$^-$, *right column*) were stained with NP396/D^b (*top row*), NRP-V7/K^d (*middle row*), or TUM/K^d (*bottom row*, negative control) tetramer. Plots are gated on CD8 T-cells; numbers in dot plots indicate the percentage of CD8 T-cells binding to tetramer. *B*: NP396/D^b (white columns) or NRP-V7/K^d tetramer–positive (black columns) CD8 T-cells isolated from the pancreas of NOD-nucleoprotein$^+$ mice were further analyzed for expression of activation markers CD62L, CD44, and CD122 (*left*) and homing marker CXCR3 (*right*). Histogram bars represent the percentage of tetramer-positive CD8 T-cells showing an activated phenotype (CD62L^{lo}CD44^{hi}CD122$^+$) (*left*) and expressing CXCR3 (*right*), respectively. Numbers above histogram bars represent the mean fluorescent intensity for CD44 gated on tetramer-positive CD8 T-cells.

by a more activated phenotype of these cells and/or different expression of homing markers, we compared expression of activation markers (CD62L, CD44, and CD122) (Fig. 4*B*, *left*) and expression of CXCR3 (Fig. 4*B*, *right*) on NP396– and NRP-V7–specific CD8 T-cells. It has been shown that activated T_H1 but not T_H2 cells express CXCR3 (27,28) and that pancreatic β-cells in NOD mice produce CXCL10, the ligand for CXCR3 (29). Therefore, increased CXCR3 expression on activated T-cells might well correlate with increased migration and accumulation of these cells into the pancreas. NP396– and NRP-V7–specific CD8 T-cells showed an activated/memory phenotype (CD62L^{lo}CD44^{hi}CD122$^+$); however, NRP-V7–specific T-cells showed stronger upregulation of CD44, which is indicative of a stronger activation/memory status (Fig. 4*B*). In addition, 40% of NRP-V7–specific but only 5% of NP396-specific CD8 T-cells expressed CXCR3 (Fig. 4*B*), and this correlated well with the higher frequencies of NRP-V7–specific T-cells found in the pancreas (Fig. 4*A*). Furthermore, the increased accumulation of NRP-V7–specific CD8 T-cells in the islets correlated well with the higher frequencies of these cells found systemically in the spleen compared with NP396-specific CD8 T-cells. Such NP396-specific CD8 T-cells were not found in the spleen of NOD-nucleoprotein transgenic mice expressing nucleoprotein in the pancreas (Fig. 3*B*), whereas NRP-V7–specific cells were detected in the spleen early, at 9 weeks of age, in NOD mice (Fig. 3*D*). Thus, differences in systemic frequencies of CD8 T-cells specific for either antigen in the spleen was reflected in differences in their frequencies in the islets, whereas identical levels were found in the pancreatic node.

NP396-specific CD8 T-cells from naïve or LCMV-infected NOD-nucleoprotein$^+$ mice show similar functional avidity. As discussed above, pancreatic NP396-specific CD8 T-cells in naïve NOD-nucleoprotein transgenic mice with pancreatic nucleoprotein expression (NOD-nucleoprotein$^+$, derived from line 6171) showed an activated phenotype (Fig. 4*B*). Hence, it was surprising that the de novo activation of NP396-specific CD8 T-cells had such a minimal impact on spontaneous diabetes, despite the fact that infection with LCMV induces rapid diabetes. We therefore analyzed whether these activated cells were also functional. We infected NOD-nucleoprotein$^+$ transgenic mice with LCMV or left them untreated and compared the ability of the different CD8 T-cell populations in the pancreas to secrete IFN-γ after a 5-h restimulation period with NP396 peptide (Fig. 5*A*). Both CD8 T-cell populations produced IFN-γ rapidly, a hallmark of antigen-experienced T-cells (Fig. 5*A*, *inset*). We then compared the functional avidity of pancreatic NP396-specific CD8 T-cells from naïve or day-7–infected NOD-nucleoprotein$^+$ mice by stimulating these cells directly ex vivo with graded doses of NP396 peptide followed by quantification of intracellular IFN-γ production. NP396-specific CD8 T-cells from naïve NOD-nucleoprotein$^+$ mice had similar functional avidity to those generated after infection with LCMV (Fig. 5*A*).

Systemic and pancreatic load of NP396-specific CD8 T-cells in NOD-nucleoprotein$^+$ transgenic mice increases strongly after infection with LCMV. We then compared the overall frequency of NP396-specific CD8 T-cells in the spleen, PDLNs, and pancreas of naive and LCMV-infected NOD-nucleoprotein$^+$ transgenic mice and included transgene-negative littermates as negative con-

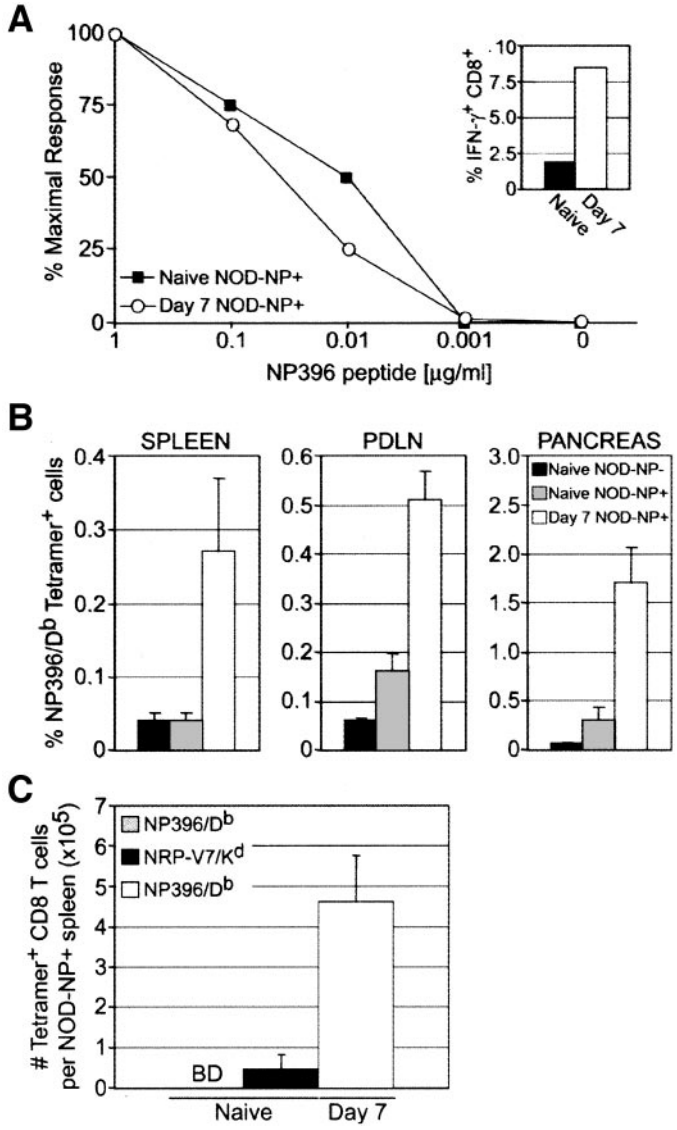

FIG. 5. LCMV infection generates much higher frequencies of NP396-specific CD8 T-cells in the spleen, PDLNs, and pancreas. Groups of NOD-nucleoprotein transgenic mice expressing nucleoprotein in the pancreas (NOD-nucleoprotein$^+$, line 6171) or transgene-negative littermates (NOD-nucleoprotein$^-$) were infected with LCMV 7 days previously or left untreated. *A*: Lymphocytes were isolated from the pancreas of naïve (black squares) or day-7 LCMV-infected (white circles) NOD-nucleoprotein$^+$ mice and were stimulated with varying concentrations of NP396 peptide for 5 h before staining for intracellular IFN-γ. To determine functional avidity regardless of the frequency of the responding T-cell populations, the number of IFN-γ$^+$ CD8 T-cells induced by peptide stimulation was expressed as a percentage of the maximum number of IFN-γ$^+$ CD8 T-cells observed after stimulation with 1 μg/ml NP396 peptide (% Maximal Response). The percentage of IFN-γ$^+$ CD8 T-cells after stimulation with 1 μg/ml NP396 peptide is shown in the *inset*, and the maximal number was quantified by relating the percentage of these cells to total numbers of CD8 T-cells in the pancreas. *B*: Lymphocytes from naïve NOD-nucleoprotein$^-$ (black bars), naïve NOD-nucleoprotein$^+$ (gray bars), or day-7 LCMV-infected NOD-nucleoprotein$^+$ mice (white bars) were isolated from the spleen, PDLNs, and pancreas and were stained with NP396/D^b tetramer. Data are graphed as the frequency of NP396/D^b tetramer$^+$ cells out of total cells. Data are an average of three mice per group for spleen and PDLNs, and three separate experiments involving groups of three mice each for pancreas, with SDs shown. *C*: The number of NP396-specific (gray bar) and NRP-V7–specific (black bar) CD8 T-cells in the spleen of naïve NOD-nucleoprotein$^+$ mice was compared with the number of NP396-specific CD8 T-cells 7 days after LCMV infection (white bar) using tetramer staining. The graph shows absolute numbers of tetramer-positive CD8 T-cells per NOD-nucleoprotein$^+$ spleen. The number of NP396-specific CD8 T-cells in the naïve NOD-nucleoprotein$^+$ spleen was below the limit of detection (BD). Data are an average of three mice per group, with SDs shown.

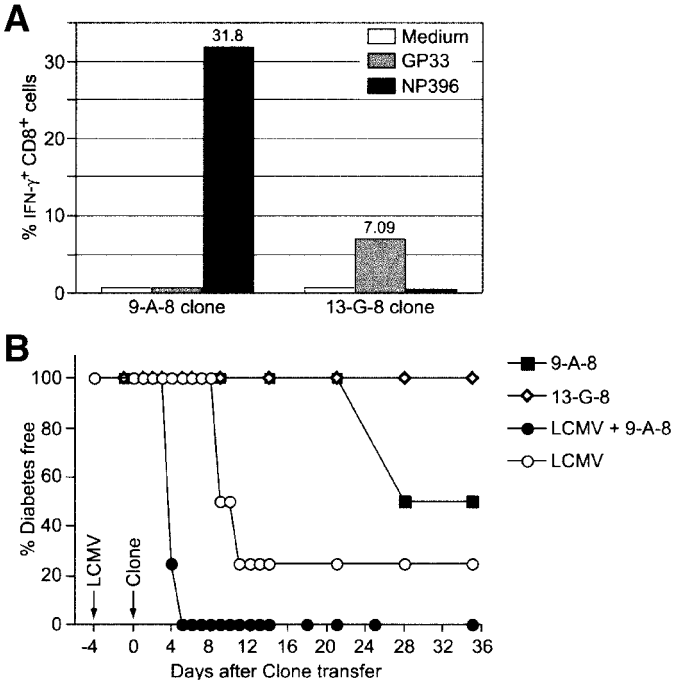

FIG. 6. Systemic increase of activated NP396-specific CD8 T-cells in NOD-nucleoprotein$^+$ mice accelerates diabetes development and increases diabetes incidence. *A*: NP396-specific T-cell clone 9-A-8 and GP33-specific CD8 T-cell clone 13-G-8 were generated from LCMV-memory NOD mice as described in RESEARCH DESIGN AND METHODS. To determine specificity and functionality of the two clones, 9-A-8 (*left*) and 13-G-8 (*right*) cells were restimulated for 5 h with irradiated macrophages loaded with GP33 (gray bars) or NP396 (black bar) peptide or left unloaded (white bars) followed by intracellular IFN-γ staining. The graph shows percentage of CD8 T-cells secreting IFN-γ. *B*: 9-A-8 and 13-G-8 T-cell clones were stimulated overnight with NP396 or GP33 peptide-loaded irradiated macrophages, respectively, followed by intravenous transfer of 3×10^5 9-A-8 (black squares, $n = 4$) or 13-G-8 (white diamonds, $n = 3$) cells into naïve NOD-nucleoprotein$^+$ transgenic mice expressing nucleoprotein in the pancreas (line 6171). In a parallel experiment, NOD-nucleoprotein$^+$ transgenic mice (line 6171) were infected with LCMV on day −4 and left untreated (white circles, $n = 4$) or received 1×10^5 9-A-8 T-cells on day 0 (black circles, $n = 4$). Mice with blood glucose values above 350 mg/dl were considered diabetic. The graph indicates percentage of mice that remained diabetes free.

trols (Fig. 5*B*). The frequency of NP396-specific CD8 T-cells in all organs tested was much higher in day 7 LCMV-infected than in naïve NOD-nucleoprotein$^+$ transgenic mice (Fig. 5*B*). This was particularly apparent in the pancreas, where LCMV infection resulted in an approximate sevenfold increase in the frequency of NP396-specific CD8 T-cells compared with those detected in naïve mice (Fig. 5*B*). Furthermore, the total number of NP396-specific CD8 T-cells generated in the spleen after LCMV infection was much higher even than those specific for NRP-V7 (Fig. 5*C*). Thus, accumulation of autoaggressive CD8 T-cells in the islets and the resulting impact on disease kinetics strongly correlates with the total number of antigen-specific T-cells present. The frequency of NP396-specific CD8 T-cells that we only found locally in the PDLNs of naïve NOD-nucleoprotein$^+$ mice was possibly too low to systemically re-circulate and significantly impact the course of the disease.

High systemic load of activated NP396-specific CD8 T-cells increases spontaneous diabetes incidence and accelerates diabetes development after LCMV-infection. We then analyzed whether systemic increase of antigen-experienced NP396-specific CD8 T-cell numbers in

naïve NOD-nucleoprotein$^+$ transgenic mice would result in diabetes induction because after LCMV infection, the number of systemic NP396-specific CD8 T-cells increased drastically and the mice developed diabetes rapidly. We therefore generated two LCMV-specific clones, NP396-specific CD8 T-cell clone 9-A-8 and GP33-specific CD8 T-cell clone 13-G-8, from LCMV-memory NOD mice as described in RESEARCH DESIGN AND METHODS. To determine specificity and function of the different CD8 T-cell clones, we restimulated the clones for 5 h with irradiated macrophages, which were left untreated or loaded with the different peptides, and we then measured intracellular IFN-γ secretion (Fig. 6*A*). NP396-specific CD8 T-cell clone 9-A-8 secreted IFN-γ after restimulation with NP396-loaded but not GP33-loaded macrophages, whereas GP33-specific CD8 T-cell clone 13-G-8 exclusively secreted IFN-γ after restimulation with GP33-loaded but not NP396-loaded macrophages (Fig. 6*A*). Specificity and functionality of NP396- or GP33-specific T-cell clones 9-A-8 and GP33 were additionally confirmed by NP396/D^b and GP33/D^b tetramer staining, respectively, and by lysis of peptide-loaded MC57 or NIT target cells (data not shown). To analyze the influence of increased systemic numbers of antigen-experienced autoaggressive T-cells on diabetes induction, T-cell clones were restimulated overnight with irradiated peptide-loaded macrophages, followed by intravenous injection of 3×10^5 NP396-specific 9-A-8 or 3×10^5 GP33-specific 13-G-8 T-cells into naïve NOD-nucleoprotein transgenic mice expressing nucleoprotein in the pancreas (NOD-nucleoprotein$^+$, derived from line 6171) (Fig. 6*B*). Four weeks after transfer of NP396-specific T-cells, one-half of the mice had developed diabetes, whereas all of the mice having received GP33-specific T-cells remained diabetes free (Fig. 6*B*). Thus, increasing systemic numbers of activated autoantigen-specific CD8 T-cells increased spontaneous diabetes incidence in naïve NOD-nucleoprotein$^+$ transgenic mice. In parallel, we analyzed the influence of higher systemic NP396-specific T-cell numbers on diabetes kinetics in an inflammatory environment, e.g., during LCMV infection. NOD-nucleoprotein$^+$ transgenic mice were infected with LCMV, and 4 days later they were either left untreated or injected intravenously with 1×10^5 NP396-specific 9-A-8 T-cells (Fig. 6*B*). NOD-nucleoprotein$^+$ mice that received NP396-specific T-cells developed diabetes faster and with a higher incidence than LCMV-infected mice that had not received T-cells (Fig. 6*B*). In summary, increasing systemic numbers of antigen-experienced NP396-specific T-cell in a naïve or inflammatory environment resulted in accelerated diabetes development and increased diabetes incidence.

DISCUSSION

Evidence presented in this report shows that introduction of a novel autoantigen into the spontaneous disease process in the NOD mouse had no significant impact on incidence of type 1 diabetes and only led to a minimal acceleration of the disease course. This was quite unexpected, because antigenic spreading is responsible for relapses in the EAE model for multiple sclerosis and was therefore thought of as a hallmark event in the pathogenesis of T-cell-mediated autoimmune disorders. One could hypothesize, based on these findings, that the autoimmune process in the NOD model is already driven by a variety of antigens at the time when nucleoprotein-specific T-cells are being activated in the PDLNs. Therefore, the impact of one additional antigen is rather limited. Conversely, attempting therapeutic elimination of antigenic specificities that behave like the response to the nucleoprotein neoantigen will probably have only a small impact in reducing disease incidence and severity, if this elimination occurs in the latter part of the pre-diabetic phase. Although the early elimination of certain autoreactive T-cells (anti–insulin-1 or anti-IGRP) by using knockout mice (13,30) or peptide treatment (17) has been successful in preventing diabetes, this might not have a high impact later during the pre-diabetic phase or in recent-onset diabetic patients. In addition, other studies have demonstrated that elimination of the T-cell response to another autoantigen, GAD, does not impact disease course (12,31).

An important consideration is that different autoantigens appear to take on differential roles in the autoimmune process. Some are suited as "drivers," whereas others act as followers, with a lesser impact on disease. The precise hierarchy might vary inter-individually and might also depend on the properties of the antigen. The intracellular compartmentalization of islet antigens, for example, might play an important role in establishing such a hierarchy. It is thus possible that only certain autoantigens are capable of inducing "driver" populations that significantly impact disease; possible examples of such autoantigens are IGRP (17) and proinsulin (32). This consideration will be important for devising immune-based preventions in type 1 diabetes, and we propose that induction of regulatory lymphocytes that can act as bystander suppressors for multiple antigenic autoaggressive specificities rather than elimination of targeted specificities might be a more effective strategy as long as the initiating autoantigens and driver epitopes, if existent, remain elusive in human type 1 diabetes pathogenesis (8,9,33,34).

We would argue that LCMV-nucleoprotein has antigenic properties that make it suitable as a driver antigen, as evidenced by the rapid diabetes onset after LCMV infection. The lack of detection of systemic NP396-specific CD8 T-cells during the spontaneous disease course but their high frequency after systemic LCMV infection in the NOD-nucleoprotein$^+$ mice is therefore surprising. The fact that the frequency of NP396-specific T-cells found in the PDLNs of responder mice was similar to the frequency of NRP-V7–specific T-cells argues that NP396 can be cross-presented efficiently. Why, however, NP396-specific CD8 T-cells were only present in ~70% of mice remains elusive and will be the subject of future studies.

It is intriguing that CD8 T-cells specific for NP396 were only found in the PDLNs at levels comparable with those specific for NRP-V7. As mentioned earlier, no NP396-specific CD8 T-cells were found in the spleen of naïve NOD-nucleoprotein$^+$ transgenic mice, whereas T-cells specific for NRP-V7 were readily detectable. Thus, there appears to be a stark difference in systemic load of CD8 T-cells generated to the nucleoprotein versus the IGRP autoantigen. This systemic difference is ultimately reflected in fourfold lower numbers of NP396-specific T-cells in the islets. One could conclude from these findings that numbers of autoaggressive CD8 T-cells generated in the PDLNs in response to autoantigens released from destroyed β-cells and transported there via lymphoid drainage of the pancreas do not necessarily correlate with disease severity. Rather, the overall systemic load of autoaggressive CD8 T-cells is indicative of their impact on the ongoing autoimmune process. This notion is supported by our finding that NRP-V7–specific CD8 T-cells in naïve

NOD and NOD-nucleoprotein$^+$ transgenic mice, as well as NP396-specific CD8 T-cells in NOD-nucleoprotein$^+$ transgenic mice after LCMV infection exhibited high systemic levels and both appeared to strongly impact the disease course (17,19) (Fig. 5). Why NRP-V7–specific T-cells are present systemically remains elusive at this point. A likely conclusion is that priming to IGRP is not only occurring in the PDLNs but also in other sites, for example, the islets themselves. This would explain their high numbers among infiltrates. However, this is not a sufficient explanation for their comparatively high frequency in the spleen. It is tempting to speculate that this is due to differences in trafficking mediated by differential chemokine receptor expression. For example, more NRP-V7–specific CD8 T-cells were found to express CXCR3 than NP396-specific T-cells. A recent report by Shigihara et al. (35) associated elevated serum CXCL10 (ligand for CXCR3) levels with type 1 diabetes progression in NOD mice. Thus, CXCR3 expression might enable NRP-V7–specific T-cells to leave the pancreas and enter the systemic circulation. In contrast, NP396-specific CD8 T-cells showed very low levels of CXCR3 expression and thus could not enter the systemic circulation. In summary, the reduced levels of CXCR3 expression and the overall lower frequencies of NP396– versus NRP-V7–specific CD8 T-cells in naïve NOD-nucleoprotein$^+$ transgenic mice might therefore well explain the lack of accelerated spontaneous diabetes. Previous reports have shown that LCMV infection induced T_C1/T_H1 responses accompanied by strong upregulation of CXCR3 on activated T_C1/T_H1 cells and early upregulation of pancreatic CXCL10 levels (36–38). These findings also explain the accelerated and high incidence of diabetes seen after LCMV infection of NOD-nucleoprotein$^+$ transgenic mice (Fig. 2*A*). LCMV infection induced strong activation and expansion of NP396-specific T-cells and upregulation of CXCR3 (Fig. 5*B*; data not shown), enabling NP396-specific T-cells to leave the pancreatic lymph node, enter the systemic circulation, and migrate toward the pancreas. This process was followed by rapid type 1 diabetes development. In the end, peripheral priming of a large number of autoaggressive CD8 T-cells, accompanied with increased CXCR3 expression, might be necessary for diabetes development.

Taken together, therapeutic elimination of only one or a few antigenic specificities will not necessarily have a major impact on an established autoimmune process, unless a driver antigen is chosen, to which high numbers of autoaggressive T-cells are generated systemically. Whether spontaneous autoimmunity in the NOD is driven by a multitude of differential specificities or a few driver clones (2) that are present in the PDLNs and islets in high numbers remains unclear. Induction and acceleration of type 1 diabetes could be the result of a simple numbers game and differential CXCR3 expression of activated autoantigen-specific T-cells, as evidenced by rapid induction of diabetes in NOD-nucleoprotein$^+$ transgenic mice after LCMV infection or after adoptive transfer of antigen-experienced NP396-specific T-cell clones.

From a therapeutic point of view, as long as autoaggressive driver specificities remain elusive, induction of bystander regulatory T-cells that can act locally in the PDLNs and affect multiple autoaggressive specificities (9) and even trigger spreading of regulatory functions (39) might be a more promising strategy than therapeutic elimination of autoaggressive T-cells.

ACKNOWLEDGMENTS

M.G.V.H. was supported by National Institutes of Health Grants AI-44451, DK-51091, and U-19 AI-51973 and by a Juvenile Diabetes Research Foundation (JDRF) grant. M.M.M. is a recipient of a Swiss National Science foundation postdoctoral fellowship. A.E.J is a recipient of a JDRF postdoctoral fellowship. D.B. is a recipient of a European Marie-Curie Outgoing fellowship.

We thank Dr. Rusung Tan (University of British Columbia, Vancouver, BC, Canada) for his kind gift of NRP-V7 and TUM tetramers and Dr. Michael Bruns for providing us with the rabbit polyclonal anti-LCMV antibody.

REFERENCES

1. McRae BL, Vanderlugt CL, Dal Canto MC, Miller SD: Functional evidence for epitope spreading in the relapsing pathology of experimental autoimmune encephalomyelitis. *J Exp Med* 182:75–85, 1995
2. Lehmann PV, Forsthuber T, Miller A, Sercarz EE: Spreading of T-cell autoimmunity to cryptic determinants of an autoantigen. *Nature* 358:155–157, 1992
3. Katz-Levy Y, Neville KL, Girvin AM, Vanderlugt CL, Pope JG, Tan LJ, Miller SD: Endogenous presentation of self myelin epitopes by CNS-resident APCs in Theiler's virus-infected mice. *J Clin Invest* 104:599–610, 1999
4. Tian J, Olcott AP, Hanssen LR, Zekzer D, Middleton B, Kaufman DL: Infectious Th1 and Th2 autoimmunity in diabetes-prone mice. *Immunol Rev* 164:119–127, 1998
5. Quinn A, McInerney B, Reich EP, Kim O, Jensen KP, Sercarz EE: Regulatory and effector CD4 T cells in nonobese diabetic mice recognize overlapping determinants on glutamic acid decarboxylase and use distinct V beta genes. *J Immunol* 166:2982–2991, 2001
6. Tian J, Lehmann PV, Kaufman DL: Determinant spreading of T helper cell 2 (Th2) responses to pancreatic islet autoantigens. *J Exp Med* 186:2039–2043, 1997
7. Garren H, Ruiz PJ, Watkins TA, Fontoura P, Nguyen LT, Estline ER, Hirschberg DL, Steinman L: Combination of gene delivery and DNA vaccination to protect from and reverse Th1 autoimmune disease via deviation to the Th2 pathway. *Immunity* 15:15–22, 2001
8. Bot A, Smith D, Bot S, Hughes A, Wolfe T, Wang L, Woods C, von Herrath M: Plasmid vaccination with insulin B chain prevents autoimmune diabetes in nonobese diabetic mice. *J Immunol* 167:2950–2955, 2001
9. Homann D, Holz A, Bot A, Coon B, Wolfe T, Petersen J, Dyrberg TP, Grusby MJ, von Herrath MG: Autoreactive CD4+ T cells protect from autoimmune diabetes via bystander suppression using the IL-4/Stat6 pathway. *Immunity* 11:463–472, 1999
10. Wong FS, Karttunen J, Dumont C, Wen L, Visintin I, Pilip IM, Shastri N, Pamer EG, Janeway CA Jr: Identification of an MHC class I-restricted autoantigen in type 1 diabetes by screening an organ-specific cDNA library. *Nat Med* 5:1026–1031, 1999
11. Liblau RS, Wong FS, Mars LT, Santamaria P: Autoreactive CD8 T cells in organ-specific autoimmunity: emerging targets for therapeutic intervention. *Immunity* 17:1–6, 2002
12. Jaeckel E, Klein L, Martin-Orozco N, von Boehmer H: Normal incidence of diabetes in NOD mice tolerant to glutamic acid decarboxylase. *J Exp Med* 197:1635–1644, 2003
13. Nakayama M, Abiru N, Moriyama H, Babaya N, Liu E, Miao D, Yu L, Wegmann DR, Hutton JC, Elliott JF, Eisenbarth GS: Prime role for an insulin epitope in the development of type 1 diabetes in NOD mice. *Nature* 435:220–223, 2005
14. Lieberman SM, Evans AM, Han B, Takaki T, Vinnitskaya Y, Caldwell JA, Serreze DV, Shabanowitz J, Hunt DF, Nathenson SG, Santamaria P, DiLorenzo TP: Identification of the beta cell antigen targeted by a prevalent population of pathogenic CD8+ T cells in autoimmune diabetes. *Proc Natl Acad Sci U S A* 100:8384–8388, 2003
15. Trudeau JD, Kelly-Smith C, Verchere CB, Elliott JF, Dutz JP, Finegood DT, Santamaria P, Tan R: Prediction of spontaneous autoimmune diabetes in NOD mice by quantification of autoreactive T cells in peripheral blood. *J Clin Invest* 111:217–223, 2003
16. Verdaguer J, Schmidt D, Amrani A, Anderson B, Averill N, Santamaria P: Spontaneous autoimmune diabetes in monoclonal T cell nonobese diabetic mice. *J Exp Med* 186:1663–1676, 1997
17. Amrani A, Verdaguer J, Serra P, Tafuro S, Tan R, Santamaria P: Progression of autoimmune diabetes driven by avidity maturation of a T-cell population. *Nature* 406:739–742, 2000
18. Yoon JW, Yoon CS, Lim HW, Huang QQ, Kang Y, Pyun KH, Hirasawa K,

Sherwin RS, Jun HS: Control of autoimmune diabetes in NOD mice by GAD expression or suppression in beta cells. *Science* 284:1183–1187, 1999
19. von Herrath MG, Dockter J, Oldstone MB: How virus induces a rapid or slow onset insulin-dependent diabetes mellitus in a transgenic model. *Immunity* 1:231–242, 1994
20. Southern PJ, Singh MK, Riviere Y, Jacoby DR, Buchmeier MJ, Oldstone MB: Molecular characterization of the genomic S RNA segment from lymphocytic choriomeningitis virus. *Virology* 157:145–155, 1987
21. Parr EL: The absence of H-2 antigens from mouse pancreatic beta-cells demonstrated by immunoferritin labeling. *J Exp Med* 150:1–9, 1979
22. Zeller W, Bruns M, Lehmann-Grube F: Lymphocytic choriomeningitis virus: X. Demonstration of nucleoprotein on the surface of infected cells. *Virology* 162:90–97, 1988
23. von Herrath MG, Guerder S, Lewicki H, Flavell RA, Oldstone MB: Coexpression of B7–1 and viral ("self") transgenes in pancreatic beta cells can break peripheral ignorance and lead to spontaneous autoimmune diabetes. *Immunity* 3:727–738, 1995
24. Christen U, Benke D, Wolfe T, Rodrigo E, Rhode A, Hughes AC, Oldstone MB, von Herrath MG: Cure of prediabetic mice by viral infections involves lymphocyte recruitment along an IP-10 gradient. *J Clin Invest* 113:74–84, 2004
25. Hudrisier D, Riond J, Burlet-Schiltz O, von Herrath MG, Lewicki H, Monsarrat B, Oldstone MB, Gairin JE: Structural and functional identification of major histocompatibility complex class I-restricted self-peptides as naturally occurring molecular mimics of viral antigens: possible role in CD8+ T cell-mediated, virus-induced autoimmune disease. *J Biol Chem* 276:19396–19403, 2001
26. Ejrnaes M, Videbaek N, Christen U, Cooke A, Michelsen BK, von Herrath M: Different diabetogenic potential of autoaggressive CD8+ clones associated with IFN-gamma-inducible protein 10 (CXC chemokine ligand 10) production but not cytokine expression, cytolytic activity, or homing characteristics. *J Immunol* 174:2746–2755, 2005
27. Sallusto F, Lanzavecchia A, Mackay CR: Chemokines and chemokine receptors in T-cell priming and Th1/Th2-mediated responses. *Immunol Today* 19:568–574, 1998
28. Loetscher M, Gerber B, Loetscher P, Jones SA, Piali L, Clark-Lewis I, Baggiolini M, Moser B: Chemokine receptor specific for IP10 and mig: structure, function, and expression in activated T-lymphocytes. *J Exp Med* 184:963–969, 1996
29. Li D, Zhu SW, Liu DJ, Liu GL: Expression of interferon inducible protein-10 in pancreas of mice. *World J Gastroenterol* 11:4750–4752, 2005
30. Moriyama H, Abiru N, Paronen J, Sikora K, Liu E, Miao D, Devendra D, Beilke J, Gianani R, Gill RG, Eisenbarth GS: Evidence for a primary islet autoantigen (preproinsulin 1) for insulitis and diabetes in the nonobese diabetic mouse. *Proc Natl Acad Sci U S A* 100:10376–10381, 2003
31. Kash SF, Condie BG, Baekkeskov S: Glutamate decarboxylase and GABA in pancreatic islets: lessons from knock-out mice. *Horm Metab Res* 31: 340–344, 1999
32. Jaeckel E, Lipes MA, von Boehmer H: Recessive tolerance to preproinsulin 2 reduces but does not abolish type 1 diabetes. *Nat Immunol* 5:1028–1035, 2004
33. Wolfe T, Bot A, Hughes A, Mohrle U, Rodrigo E, Jaume JC, Baekkeskov S, von Herrath M: Endogenous expression levels of autoantigens influence success or failure of DNA immunizations to prevent type 1 diabetes: addition of IL-4 increases safety. *Eur J Immunol* 32:113–121, 2002
34. Coon B, An LL, Whitton JL, von Herrath MG: DNA immunization to prevent autoimmune diabetes. *J Clin Invest* 104:189–194, 1999
35. Shigihara T, Oikawa Y, Kanazawa Y, Okubo Y, Narumi S, Saruta T, Shimada A: Significance of serum CXCL10/IP-10 level in type 1 diabetes. *J Autoimmun* 26:66–71, 2006
36. Seewaldt S, Thomas HE, Ejrnaes M, Christen U, Wolfe T, Rodrigo E, Coon B, Michelsen B, Kay TW, von Herrath MG: Virus-induced autoimmune diabetes: most beta-cells die through inflammatory cytokines and not perforin from autoreactive (anti-viral) cytotoxic T-lymphocytes. *Diabetes* 49:1801–1809, 2000
37. Christen U, McGavern DB, Luster AD, von Herrath MG, Oldstone MB: Among CXCR3 chemokines, IFN-gamma-inducible protein of 10 kDa (CXC chemokine ligand (CXCL) 10) but not monokine induced by IFN-gamma (CXCL9) imprints a pattern for the subsequent development of autoimmune disease. *J Immunol* 171:6838–6845, 2003
38. Christensen JE, de Lemos C, Moos T, Christensen JP, Thomsen AR: CXCL10 is the key ligand for CXCR3 on CD8+ effector T cells involved in immune surveillance of the lymphocytic choriomeningitis virus-infected central nervous system. *J Immunol* 176:4235–4243, 2006
39. Alpan O, Bachelder E, Isil E, Arnheiter H, Matzinger P: 'Educated' dendritic cells act as messengers from memory to naive T helper cells. *Nat Immunol* 5:615–622, 2004